OCLC FirstSearch: Display

Your requested information from your library   NATIONAL MARINE FISHERIES, PAN

Return

PENDING - Lender

51481771

GENERAL RECORD INFORMATION			
Request Identifier:	51481771	**Status:**	PENDING 20090302
Request Date:	20090302	**Source:**	ILLiad
OCLC Number:	14100627		
Borrower:	FTU	**Need Before:**	20090401
Receive Date:		**Renewal Request:**	
Due Date:		**New Due Date:**	
Lenders:	*FD6, MXF, NOC, NOC, FEC		
Request Type:	Copy		

BIBLIOGRAPHIC INFORMATION

Call Number:	
Uniform Title:	Trends in ecology & evolution (Personal ed.)
Title:	Trends in ecology & evolution.
ISSN:	0169-5347
Imprint:	Amsterdam [Netherlands] : Elsevier Science Publishers B.V. , c1986-
Article:	Sugihara and May: Applications of fractals in ecology.
Volume:	5
Number:	3
Date:	1990
Pages:	79-86
Verified:	<TN:263531><ODYSSEY:132.170.184.20/ILL> OCLC

MY LIBRARY'S HOLDINGS INFORMATION

LHR Summary:	v.1-(1986-)
Lending Policies:	Unknown / Unknown
Location:	FD6A
Format:	unspecified

BORROWING INFORMATION

Patron:	Weishampel, John
Ship To:	University of Central Florida Library/Interlibrary Loan/P.O. Box 162430/4000 Central Florida Blvd/Orlando, FL 32816-2430 //ARIEL 132.170.184.250
Bill To:	Same; FEIN 592-924-021
Ship Via:	ARIEL/BOOK RATE / DLLI
Electronic Delivery:	Odyssey - 132.170.184.20/ILL
Maximum Cost:	IFM - 25.00
Copyright Compliance:	CCL
Billing Notes:	IFM preferred; invoice OK
Fax:	407-823-3047 (fax) / 407-823-5422 (phone)
Email:	illbor@mail.ucf.edu
Affiliation:	DLLI/CFLC/FLIN/SOLINE (SO6)/ASERL Reciprocal//Thank you!
Borrowing Notes:	

References

1 Thomas, P.A. and Room, P.M. (1986) *Nature* 320, 581–584
2 Bennett, F.D. (1966) *Proc. South. Weed Conf.* 19, 497–504
3 Mitchell, D.S. (1972) *Br. Fern Gaz.* 10, 251–252
4 Forno, I.W. and Harley, K.L.S. (1979) *Aquat. Bot.* 6, 185–187
5 Forno, I.W. (1983) *Aquat. Bot.* 17, 71–83
6 Whitham, T.G. and Slobodchikoff, C.N. (1981) *Oecologia* 49, 287–292
7 Room, P.M. (1988) *J. Ecol.* 76, 826–848
8 Room, P.M. and Thomas, P.A. (1986) *J. Appl. Ecol.* 23, 1013–1028
9 Julien, M.H., Bourne, A.S. and Chan, R.R. (1987) *J. Appl. Ecol.* 24, 935–944
10 Julien, M.H. and Bourne, A.S. (1988) *J. Appl. Entomol.* 106, 518–526
11 Southwood, T.R.E. (1977) *J. Anim. Ecol.* 46, 337–365
12 Grime, J.P. (1979) *Plant Strategies and Vegetation Processes*, Wiley
13 Baker, H.G. (1965) in *The Genetics of Colonising Species* (Baker, H.G. and

Stebbins, G.L., eds), pp. 147–172, Academic Press
14 Feeny, P. (1976) *Recent Adv. Phytochem.* 10, 1–40
15 Julien, M.H. (1987) *Biological Control of Weeds: A World Catalogue of Agents and their Target Weeds*, CAB International
16 Forno, I.W. (1981) in *Proc. 5th Int. Symp. Biol. Control Weeds (Brisbane 1980)* (Del Fosse, E.S., ed.), pp. 167–173, CSIRO
17 Sands, D.P.A., Schotz, M. and Bourne, A.S. (1986) *Entomol. Exp. Appl.* 42, 231–237
18 Room, P.M. and Thomas, P.A. (1985) *J. Appl. Ecol.* 22, 139–156
19 Strong, D.R., Lawton, J.H. and Southwood, T.R.E. (1984) *Insects on Plants: Community Patterns and Mechanisms*, Blackwell Scientific
20 Room, P.M., Harley, K.L.S., Forno, I.W. and Sands, D.P.A. (1981) *Nature* 294, 78–80
21 Calder, A.A. and Sands, D.P.A. (1985) *J. Aust. Entomol. Soc.* 24, 57–64
22 Taylor, M.F.J. (1988) *J. Anim. Ecol.* 57, 873–891
23 Julien, M.H. and Bourne, A.S. (1986) *Oecologia* 70, 250–257
24 Forno, I.W. and Semple, J.L. (1987) *Oecologia* 73, 71–74
25 Forno, I.W. and Bourne, A.S. (1988) *Z. Angew. Entomol.* 106, 85–89
26 Taylor, M.F.J. and Forno, I.W. (1987) *Z. Angew. Entomol.* 104, 73–78

27 Room, P.M. (1986) in *Proc. EWRS/AAB 7th Symp. Aquat. Weeds* (Peterse, A.H., ed.), pp. 271–276, European Weed Research Society
28 Doeleman, J.A. (1989) *Biological Control of Salvinia molesta in Sri Lanka: An assessment of Costs and Benefits*, ACIAR Technical Report 12
29 Waage, J.K. and Greathead, D.J. (1988) *Philos. Trans. R. Soc. London Ser. B* 318, 111–128
30 Scriber, J.M. and Slansky, F. (1981) *Annu. Rev. Entomol.* 26, 183–211
31 Room, P.M. and Thomas, P.A. (1986) *Aquat. Bot.* 24, 213–232
32 Room, P.M., Julien, M.H. and Forno, I.W. (1989) *Oikos* 54, 92–100
33 Semple, J.L. and Forno, I.W. (1987) *J. Aust. Entomol. Soc.* 26, 365–366
34 Kuno, E. (1987) *Adv. Ecol. Res.* 16, 249–337
35 May, R.M. and Hassell, M.P. (1988) *Philos. Trans. R. Soc. London Ser. B* 318, 129–169
36 Wapshere, A.J. (1985) *Agric. Ecosys. Environ.* 13, 261–280
37 Schlettwein, C.H.G. (1985) *Madoqua* 14, 291–293
38 Rozenzweig, M.L. (1971) *Science* 171, 385–387
39 Room, P.M. (1986) in *The Ecology of Exotic Animals and Plants* (Kitching, R.L., ed.), pp. 164–186, John Wiley & Sons

Applications of Fractals in Ecology

George Sugihara and Robert M. May

Fractal models describe the geometry of a wide variety of natural objects such as coastlines, island chains, coral reefs, satellite ocean-color images and patches of vegetation. Cast in the form of modified diffusion models, they can mimic natural and artificial landscapes having different types of complexity of shape. This article provides a brief introduction to fractals and reports on how they can be used by ecologists to answer a variety of basic questions about scale, measurement and hierarchy in ecological systems.

A biophysicist creates a geometric model of a spruce tree by approximating its shape as a cone perched on top of a cylinder. An elm leaf becomes an ellipse and seed shadows are conveniently mapped as discs of varying diameters covering a landscape. Until recently, such discussions of the shape and measure of natural objects have relied heavily on simplifying assumptions about the underlying geometry, replacing the acknowl-

George Sugihara is at the Scripps Institution of Oceanography A-002, University of California, San Diego, La Jolla, CA 92093, USA; Robert May is at the Dept of Zoology, South Parks Road, Oxford OX1 3PS, UK.

edged complexity of real-world objects by simplified euclidean ideals.

There is, however, growing recognition that many natural objects have a graininess or nested irregularity to them, which places them within the realm of fractal geometry. Whereas in the euclidean scheme lines are smooth, in fractals lines are jagged (not differentiable), often exhibiting a special type of self-similar structure that is repeated on different scales. As Mandelbrot[1] has emphasized, this peculiar kind of nested irregularity, which appears to be so ubiquitous in nature, can become a source of simplicity when fractal methods are applied (see, for example, Fig. 1).

Fractals are based on the idea that any measure that we assign to an object (e.g. the amount of length, area, volume, etc.) depends on some notion about appropriate dimensions. Thus, for example, a line has zero area (planar measure), whereas a plane has infinite length (because it would take a line of infinite length folded back on itself to fill it). At first glance, the problem

of choosing appropriate units for measurement may seem trivial, but, as we shall see, for many natural objects having complicated shapes this is not the case. In fact, problems as apparently simple as measuring the length of a coastline or the area of available leaf habitat for insects can be rather tricky insofar as they have fractal geometry. Although the technical origins of fractals in measure theory may seem abstruse (e.g. Ref. 3), the basic ideas of fractal analysis are extremely simple and intuitive, and one can begin to work with them very quickly.

This review gives an introduction to fractal techniques, pointing out possible applications in ecological research. It begins with an informal discussion of the theory of fractals, followed by a section providing details on specific methods of computing them. This is then followed by a survey of possible field applications, which are intended to illustrate the utility of fractals in ecological research (Ref. 4 and Sugihara, unpublished), and particularly their use as a tool for
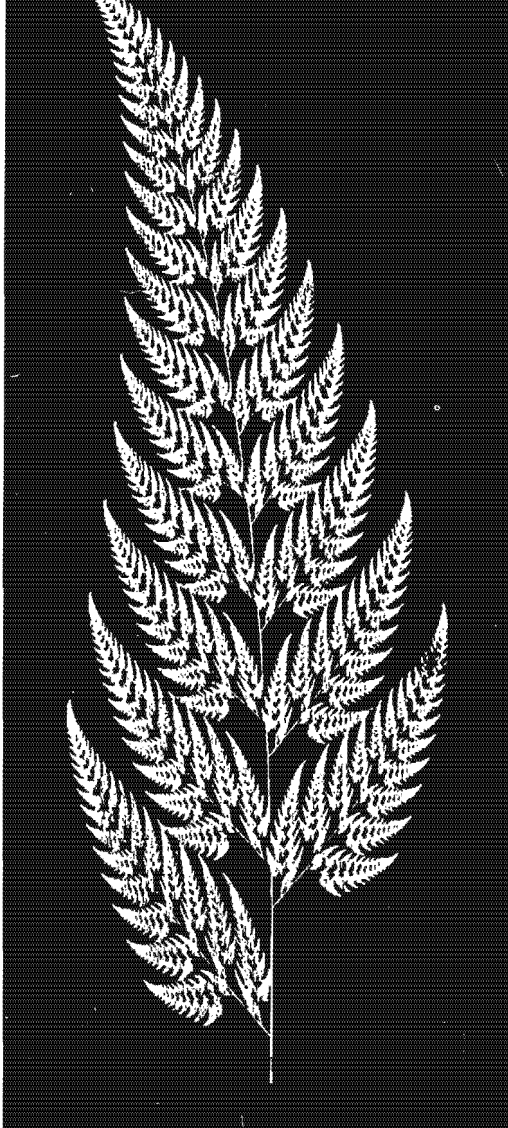
Fig. 1. Fractal image of a black spleenwort fern produced by a model consisting of four simple transformations each having only six parameters (*from Ref. 2, with permission*). By contrast, a euclidean description of this complex shape might involve a polynomial involving thousands of fitted parameters.

addressing problems of scale and hierarchy[5-10]. For a more detailed review of these ideas, with some

different examples of applications in ecology, see Frontier[11].

Defining a fractal dimension
How long is the coastline of Britain?

Suppose the jagged curve in Fig. 2a represents a section of coastline. How long will it take me to walk this coastal path; how long is this jagged coastline? To measure with a ruler, I could approximate the length of the curve with a polygonal arc having N straight-line segments, each of length δ, as shown in Fig. 2b. One could think of realizing this measurement scheme by using dividers set to width δ, and flipping the dividers along the curve. The total estimated euclidean length of the curve, L, would be the number of sides of the polygon, N, multiplied by the length of each side, δ. But as I move to finer scales – to shorter straight-line segments, having smaller values of δ; to more finely-set dividers – I will be able to trace the wiggly ins and outs of the coastline more closely. Thus, the length of the coastline will increase as I measure it on finer and finer scales.

In practice, the lengths, L, of many interesting objects in the natural world – coastlines, rivers, tree trunks, and so on – are found to depend on measurement scale, δ, according to a simple power law (over an appropriate range of δ values):

$$L(\delta) = K\delta^{1-D} \qquad (1)$$

Here L is the length, measured on the characteristic scale δ, and the exponent D is called the 'fractal dimension' $(2 > D > 1)$.

Figure 3 gives some examples of such 'coastlines', along with their fractal dimensions. For the familiar

euclidean geometry that we were all brought up to know and love, $D=1$. That is, the length is simply a constant, $L=K$, independent of measurement scale. More generally, for geometrical objects such as 'Koch's snowflake' (Fig. 3b and Box 1), the structure of the outline of the object repeats itself on finer and finer scales; successive magnifications of the object show the same 'self-similar' structure. As shown in Box 1, the fractal dimension of Koch's snowflake is $D = 1.26$.

In the natural world, there is no guarantee that such elegant self-similar properties will apply. Although coastlines, landscape patterns, vegetation boundaries, leaf perimeters and the like do show fractal geometric patterns, the characteristic fractal dimension, D, of Eqn 1 may – as we shall see below – itself change with changes in the measurement scale, δ.

D as a measure of complexity

Box 2 gives a brief indication of the relationship between the essentially intuitive presentation of ideas about fractal geometry in this review and their more formal origins in measure theory. One of the problems with an excessively intuitive approach is that it invites the suggestion that maybe the coastline of Britain *is* a defined entity, and that what we are fussing about is only a problem of practicality of measurement. Koch's snowflake and other such self-similar geometrical objects make it clear that something deeper is at stake: for such abstract objects, boundary lengths become infinite as δ tends to zero (at a rate determined by Eqn 1). For real objects, there will be physical limitations to the minimum meaningful scale (ultimately set by molecular dimensions, but usually by other commonsense considerations before that). But the problem is nevertheless deeper than one of trivial measurement accuracy; a tree trunk literally has larger and larger circumference as one moves to smaller and smaller scales, in a manner characterized by Eqn 1, and this has consequences for the way the tree trunk looks to creatures of different sizes.

More explicitly, consider Eqn 1 applied to a coastline for which $D=1.5$. Here, a tenfold reduction in measurement scale will increase the
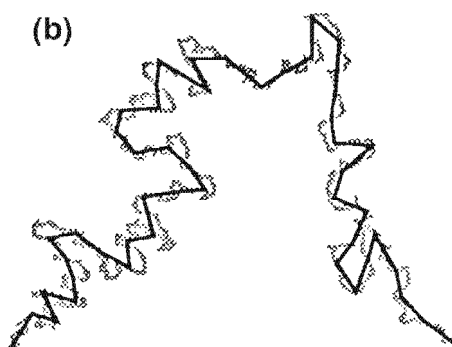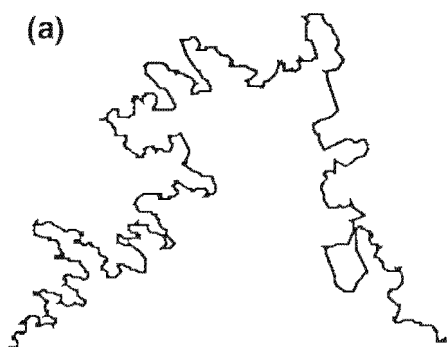

Fig. 2. (a) An irregular curve. (b) The length of the curve is measured using a polygonal approximation, where curve length is reckoned as the number of sides $(K \delta^{-D})$ times the length of each side (δ); K is a constant (see Box 2) and D is the 'fractal dimension'. In a fractal curve, measured length $(L(\delta) = K \delta^{1-D})$ grows as δ declines (cf. Eqn 1).

apparent length by a factor of $10^{0.5} \approx 3$. In general, we see from Eqn 1 that the faster the apparent length changes as measurement scale changes, the larger D becomes.

For an ideally smooth and simple curve, the fractal dimension $D = 1$ is equal to the formal 'topological dimension', D_T, that we expect 'one-dimensional' objects to have. But for the jagged curves that we have been discussing, D will exceed D_T; a more formal definition of Mandelbrot's fractal forms are those where D exceeds D_T.

Returning to the curves in Fig. 3, we notice explicitly that larger values of D correspond to curves that are increasingly complex. In the case of the Brownian trail in the plane, for example, the curve is so complex as to literally fill the plane (which is why we did not draw it!); that is, for this Brownian trail in the plane, $D = 2$; see Box 3.

The fractal exponent, therefore, describes the complexity of a shape. Moreover, this complexity of shape is reflected in the speed with which apparent length changes as measurement scale changes. For larger values of D, length changes faster because the curve is more complex.

Measuring the fractal dimension, D
Dividers method (boundary dimensions: $2 > D > 1$)

This method involves stepping along a curve or boundary with dividers to see how apparent length, $L(\delta)$, changes as the dividers are brought closer together. Using a spectrum of widths of dividers, one plots log L versus log δ and determines D according to Eqn 1 as 1.0 minus the slope of the linear regression through these points; see Box 2. Again, the fractal exponent D can only be thought of as a Hausdorf dimension in the limit as the divider width goes to zero, $\delta \rightarrow 0$. This, of course, can never be realized in practice because the so-called 'inner scale' of measurement of D will be constrained by such things as the resolution of the photographic image or of the dividers.

In practice, for a given δ, it is a good idea to repeat the exercise starting from a variety of different points on the curve, because L will have some variance to it depending on where on the curve one starts. In this way, one can either construct a

plot of log L versus log δ containing more points, or obtain a distribution of D values. An additional complication, to be discussed below, is the possibility that D may change abruptly at some measurement scale; that is, for a particular range of δ we may obtain one value of D whereas at another scale range we obtain a new value of D.

Grid method (boundary dimension)

If the landscape image or other object is digitized on a plane, it is easier to use the following approximation based on the equations in Box 2. Superimpose on the image a regular grid, composed of squares of side length δ. At some δ, count the number of grid squares containing a piece of the curve or boundary and call this C (in technical jargon, the grid squares form an approximate δ-cover over the curve). Repeat this for various δ, and compute D as the magnitude of the slope of the regression line through a plot of log C verus log δ (to be pedantic, D is (-1) times this slope). Reorienting the grid relative to the image has the same effect that choosing different starting points has in the divider method (see also the discussion of pointwise dimension by Gukenheimer[13]).

Grid method (general)

If the image is digitized and embedded in N dimensions (as will be the case, for example, if the image is a strange attractor in a high-dimensional phase space), then D may be computed as in the preceding paragraph by using an N-dimensional grid of boxes of side length δ to cover the object. For various values of δ, the log of the number of N-dimensional boxes containing a piece of the object (log C) is plotted against log δ. Again following the equation in Box 2, D may be estimated as the slope of the regression of log C against log δ as $\delta \rightarrow 0$. Note that if the shapes are planar islands and the interior points are included in C, then D should equal 2 in the limit as $\delta \rightarrow 0$. At larger values of δ, the boundary irregularities may predominate so that D may appear to be less than 2.

Perimeter/area method (boundary dimension)

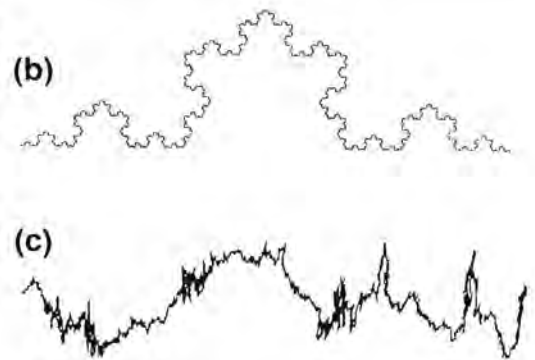If the object consists of a mosaic of irregular islands (for instance, im-

(b)

(c)

Fig. 3. A higher fractal dimension is associated with higher shape complexity. (a) A straight line, $D = 1$. (b) Koch curve, $D = \log 4 / \log 3$; see Box 1. (c) Brownian time series (line-to-line function), $D = 1.5$. A Brownian trail in the plane (not shown) is 'plane-filling' and consequently $D = 2$; see Box 3.

ages of ocean colours or vegetation patches) the dimension of the boundaries of these islands can be estimated from perimeter/area data, by using the relation $P = A^{D/2}$. That is, one calculates the perimeter, P, and area, A, of each irregular tile at some fixed δ, and plots these values on log coordinates so that the slope of the regression is equal to $D/2$. The choice of δ should not affect the result, as long as the objects are simple fractals generated by rules of self-similarity; in such situations, the plot of log A against log P will give a single straight line, providing a unique D

**Box 1. The fractal dimension of Koch's snowflake**

Koch's snowflake is constructed by the following rule. Start with an equilateral triangle. Take the middle third of each side, and replace it with the other two sides of an equilateral triangle (smaller, of course, than the original one) pointing outward. Now do this again to each line segment in the new figure. And again, indefinitely many times, repeating the same process on smaller and smaller scales. Figure 3b shows one of the three sides of the ensuing 'snowflake'.

The snowflake has an area not much larger than that of the original equilateral triangle. But how large is its perimeter? Each step in the process obviously lengthens the perimeter by a factor 4/3, so the asymptotic perimeter is $(4/3) \times (4/3) \times \ldots$, which is infinite!

To characterize the fractal dimension of the snowflake, look at Eqn 1 in the main text. Each step in the recipe represents reducing the measurement scale by a factor of 3 ($\delta_{n+1}/\delta_n = 1/3$) and consequently increasing the length by a factor of 4/3 [$L(\delta_{n+1}) / L(\delta_n) = 4/3$]. Substituting into Eqn 1, we have

$$4/3 = (1/3)^{1-D}$$

That is, $4 = 3^D$, or $D = \ln 4 / \ln 3 = 1.26$.

Box 2. Measure theory, Hausdorf dimension and fractal dimension
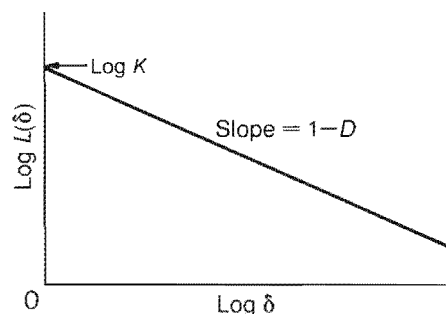
The graph is a plot of log apparent length, $L(\delta)$, on log divider's width (δ). For a fractal curve, the log apparent length grows linearly as the dividers are brought closer together (logarithmically). The slope of the line is $1 - D$.

This illustrates Eqn 1, applied to a self-similar, fractal object (for example, Koch's snowflake) for which D is indeed a constant. A question asked by measure theory is to find some relative measure (for a given dimension, D) that does not depend on the scale, δ. Hausdorf proposed the parameter K, the asymptotic intercept with the y-axis in the plot, as such a measure.

Alternatively, we may return to the measurement procedure in Fig. 1, and note that for such a polygonal approximation to an irregular curve, the approximate linear measure K may be calculated by adding up the sides' lengths, δ, after they are each raised to the power D [more specifically, Eqn 1 tells us that the number of sides of the polygon is $N = K\delta^{-D}$, where each side has a 'D-dimensional length' δ^D, so that the approximate measure is $(K\delta^{-D})\,\delta^D = K$].

Expanding on this theme, we see that if a linear measurement scales as n, then a D-dimensional measurement scales as $k = n^D$. Thus, if an object of dimension D is expanded by increasing its linear size in each spatial dimension n times, then its volume (D-dimensional measurement) is increased by a factor of $k = n^D$ times the original. This simple scaling relationship, $k = n^D$, thus suggests the following general notion of dimension:

$$D = \ln k \,/\, \ln n$$

where k is the multiple by which the D-dimensional measurement (e.g. volume) increases, and n is the multiple by which the corresponding linear measurement increases. We call this D the fractal dimension or fractal exponent; it is the same D as met in Eqn 1.

According to these intuitive arguments, the fractal exponent is an allometric scaling constant that behaves something like a dimension. To interpret this exponent more rigorously as the Hausdorf dimension requires that we investigate the scaling as the linear measurement, δ, approaches zero. That is, the Hausdorf dimension may be defined as

$$D_h = \text{limit } [\ln C \,/\, \ln (1/\delta)] \quad \text{as } \delta \to 0$$

Here C is, for example, the number of sides in the polygon (more generally, C is the 'cardinality of a minimal δ-covering of the set'). Thus, as in the more intuitive approaches, we are looking at how apparent length changes with respect to scale, but now we are doing so in the limit $\delta \to 0$. If the plot of $\ln L$ versus $\ln \delta$ is really linear for all δ, as suggested by Eqn 1, then the Hausdorf dimension and the fractal exponent are equal, $D = D_h$.

In practice, D_h can never really be obtained because of the finite resolution of measuring instruments or photographic grain. Moreover, given this constraint, it is most plausible that as $\delta \to 0$ the Hausdorf dimension will equal unity for most natural outlines. Largely for this reason, but also because fractal ideas are easier to grasp intuitively, we focus the discussion in this review on D rather than D_h.

---

for all δ of interest. More generally, D itself may depend on the scale of measurement, as reflected in the characteristic magnitude of P or A.

Notice that D obtained in this way is an ensemble measure for the collection of islands or patches. This is in contrast to the previous methods, which can be applied to the boundary of a single island.

Hyperbolic distribution (boundary dimension)

Certain rules or mechanisms that generate archipelagoes of self-similar islands (for instance, so-called Koch islands) are known to produce size–frequency distributions that are hyperbolic:

$$\Pr(A > a) = ca^{-B} \qquad (2)$$

Here $\Pr(A > a)$ stands for the probability that the area of a given island, A, will exceed some specified value, a; c and B are positive constants. Hyperbolic distributions of areas have been demonstrated empirically for patches of vegetation[12], the Aegean Islands[14], and global landmasses[1]. Mandelbrot[1] suggests that – under certain assumptions about the generating mechanism – it may be possible to fit a hyperbolic distribution to data on island areas, and by so doing to obtain an estimate of D for island boundaries. In particular, when the generating mechanism has a specific geometric form, it can be shown that $D = 2B$. It follows that archipelagoes composed of irregularly shaped islands will tend to be dominated by many small islands

(as exemplified by the Baltic coast of Sweden or Finland).

Like the perimeter/area method, this distribution-based estimate is of course an ensemble measurement, but all that is required here is the area of each tile, measured at some fixed value of δ. When applied to global landmasses, Mandelbrot[1] finds that this method gives estimates of D between 1.2 and 1.3, which accords with estimates obtained by the dividers method.

Ecological applications
Measuring habitat space

One of the more straightforward applications of the notions of fractal dimension and fractal measure in ecology is to the problem of measuring available habitat space.

Morse et al.[15] have applied these methods to the question of why in a given habitat there tend to be so many more individuals of small animals than of larger ones. They investigate this question for arthropods living on vegetation whose surface area is believed to be fractal; that is, whose surface area appears to expand at finer and finer scales. Using photographs of various types of vegetation, they calculate a value for the fractal dimension of the habitat flora by the boundary-grid method. They find a value of D between 1.3 and 1.5, which pertains to the outlines of the planar projections of the vegetation in the photographs. Taking the approximation that $D \approx$ 1.5 for the leaf boundaries, heuristic upper and lower bounds on D for the surfaces are $2 \times 1.5 = 3$ and $1 + 1.5 = 2.5$ (cf. Ref. 16, p. 365). Following Eqn 1, this means that for an order of magnitude decrease in ruler length (δ) the perceived surface area of vegetation increases between 3.16 and 10 times. Thus, organisms that are an order of magnitude smaller in length would have between 3.16 and 10 times more available living space. Moreover, the observed fractal scaling of the vegetational substrate, which provides small arthropods with much more living space than is available to larger ones on the same substrate, is qualitatively consistent with predictions of individual abundance based on allometric arguments. Morse et al.[15] speculate that the steep increase observed in the abundance of arthropods as body size decreases, is qualitatively con-

sistent with predictions based on the fractal scaling of the vegetation on which they live.

Briand and Cohen[17] discuss habitat dimensionality in relation to food web shape, suggesting that webs from three-dimensional habitats are longer and narrower than webs from planar habitats. Only rough arguments are made in guessing the dimensionality of habitats, and criticisms have been made[10,18] that the apparent differences seen may in fact be a more accurate reflection of the differences in data collection habits of investigators studying aquatic versus terrestrial environments. Although it has yet to be tried, fractal methods could conceivably be applied to resolve this problem. Measurements of D for environments of a given type could be used to determine whether within a given web type the presumed trend with dimension still exists. Thus, one might use photographs to measure the fractal dimensions of the environments from which each web was drawn. Alternatively, the D-dimensional measure for available habitat space in each environment may be a more important quantity for regulating food web shape. Thus, fractals can be used to compare webs of a given type by providing a quantifiable continuum for habitat dimension and measure.

Dimension as a function of scale: detecting functional hierarchies

By definition, the Hausdorf dimension involves computing the unique value $D_h = \log C / \log \delta$ in the limit as $\delta \rightarrow 0$ (see Box 2). Notice that D_h is independent of length scale, δ. As suggested in Box 2, in most applications it is more useful to adopt the less formal sense of dimension given by the fractal exponent, $D = \log k / \log n$, where D may in fact depend on the *inner* and *outer* scales of measurement (a particular range of δ for which a straight line is obtained on a log–log plot). Mandelbrot provides a nice example of this idea in discussing how a ball of string appears to change dimension depending on how close the observer is. As the ball is approached from afar the string goes through the sequence of dimension changes, 0 (a distant point), 3 (a closer ball), 1 (the linear thread), 3 (the three-dimensional tubular thread), etc., illustrating how

apparent dimension may change with observational scale (i.e. different ranges of δ). Different observational scales capture different aspects of structure, and these transitions are signaled by shifts in the apparent dimension of the object. This latter fact suggests an interesting application of fractals as a method for distinguishing hierarchical size scales in nature.

A constant fractal exponent over a given size range (inner and outer scale) may indicate that within

this region large-scale features are simply magnified versions of smaller ones. As discussed above, such constant scaling could be produced by a single (possibly complex) self-similar generating process. It should be required, moreover, if one is trying to extrapolate mechanisms from small scale to large.

On the other hand, a shift in D at the inner or outer scale may indicate a shift in generating process, and define a boundary across which one may no longer make extrapolations.

Box 3. Inferring dynamics from complexity of shape: a Brownian neutral model

The important connection between fractal patterns and self-similar generating processes can be made more explicit by considering modified Brownian diffusion processes. Mandelbrot[1] and Hastings et al.[12] have discussed how fractal exponents may be incorporated into diffusion processes, as a scaling factor for normalizing increments in space and time. This normalization effectively tunes the memory of a diffusion process, to produce either smoother ('persistent') or more complex ('anti-persistent') outlines characterized by their fractal complexity.

A modified Brownian process is defined in terms of some random variable characterizing displacement, $X(t)$, which is distributed as Gaussian white noise, with a root mean square equal to

$$\text{r.m.s. } X(t) = (\triangle t)^H$$

Depending on the value of H, the process can be said to be positively or negatively correlated. When $H = 1/2$, the process is classical Brownian motion, with no serial correlation between the displacements in successive time intervals. This means that, at every stage and at every scale of $\triangle t$, all directions of displacement are equally likely. If $1 > H > 1/2$, the increments of displacement may be roughly thought of as overlapping each other, above time increments that do not overlap. Such a process may be said to be positively correlated, or persistent, in the sense that a particle moving in some direction at time t will tend to move in the same direction regardless of $\triangle t$. Roughly speaking, the grain of the Brownian path will have been smoothed out in a statistically self-similar fashion that transcends all scales.

To summarize, the H values for constrained white noise may be characterized as:

$H = 1/2$, Brownian
$H > 1/2$, Persistent
$H < 1/2$, Anti-persistent

These results translate to fractal curves and landscapes. Smoother curves can be generated by higher values of H, and more irregular curves by lower values. The classical Brownian value, $H = 1/2$, serves as a neutral value.

Mandelbrot[1] and Hastings and Sugihara (unpublished) have shown that the exponent H can be related to the fractal exponent, D, with the precise relationship depending on the details of the Brownian generating model. If the process involves a Brownian trail in the plane (a Brownian line-to-plane function), say for describing animal movements in two dimensions, then D for the resulting path can be shown to be

$$D = 1/H$$

Thus, for the classical Brownian trail where $H = 1/2$, we find that $D = 2$; the curve effectively fills the plane. Adding persistence to the modified random walk smooths the trail out and lowers the dimension; the curve becomes less plane-filling.

If the process involves level curves cutting across a crinkled Brownian sheet (e.g. isoelevation lines on a topographic map; a Brownian plane-to-line function), or if we are considering the time series of a Brownian process (displacement versus time; a Brownian line-to-line function), then D may be calculated from the relation

$$D = 2 - H$$

Conversely, we can use the above relationships to infer the H value required in order that the appropriate Brownian process may reproduce the texture of an observed random fractal pattern. That is, one can infer the space–time scaling that would be required of a modified Brownian model to approximate the texture of the observed fractal pattern. Mandelbrot[1] provides some nice examples of this.
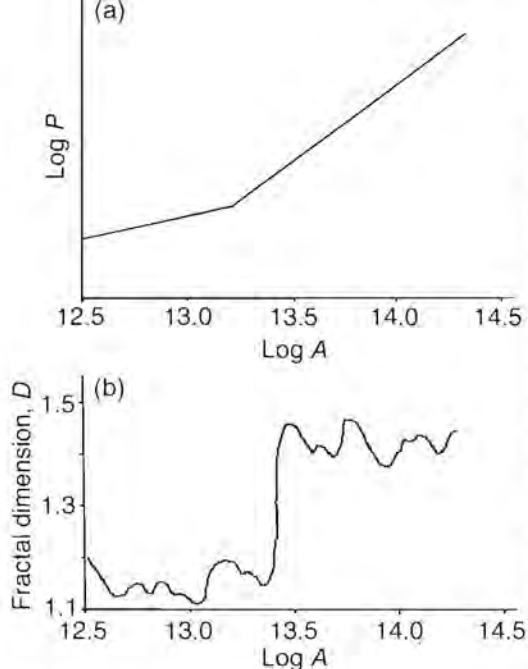
Fig. 4. (a) A plot of log patch perimeter (*P*) against log patch area (*A*) for aerial photographs of deciduous forest in Natchez Quadrangle, Mississippi, USA. (b) Using a sliding window of 60 points along the *x*-axis, a discontinuity in *D* is uncovered at 60–70 ha; this is marked by a kink in the curve at this scale. Such kinks indicate shifts in dimension, and may demarcate boundaries between hierarchical levels. *From Ref. 19, with permission.*

In this way, fractals may provide a methodology for obtaining objective answers to such difficult problems in hierarchy theory as how to determine boundaries between hierarchical levels and how to determine the scaling rules for extrapolating within each level (Ref. 19 and Sugihara, unpublished).

Bradbury *et al.*[20] investigate the possibility of hierarchical scaling in an Australian coral reef. They use the dividers method in transects across the reef to determine whether *D* (boundary) depends on the range of length scales. They find that *D* declines abruptly from a value of about 1.1 at the finest scale (δ = 10 cm) to a value of about 1.05 for intermediate lengths (δ between 20 cm and 200 cm), and rises sharply to a value of about 1.15 at the largest scales (δ between 5 m and 10 m). Again, the constant *D* within each of these size ranges suggests the possibility of a single class of processes for generating reef structure that are self-similar within these size ranges. The shifts in *D* between scaling intervals indicate when the processes are different at each scale. These three ranges of scale correspond nicely with the scales of three major reef structures: 10 cm

corresponds to the size of anatomical features within individual coral colonies (branches and convolutions); 20–200 cm corresponds to the size range of whole adult living colonies; and 5–10 m is the size range of major geomorphological structures such as groves and buttresses. That is to say, the shifts in fractal exponent at different scales appear to signal where the breakpoints occur in the hierarchical organization of reefs.

In similar vein, Krummel *et al.*[19] evaluate the fractal dimension of deciduous forest patterns in Mississippi using the perimeter/area method on aerial photographs of the US Geological Survey (1973) Natchez Quadrangle. This region has experienced relatively recent conversion of native forests into agricultural use. Repeated calculations of *D* using a sliding window of 60 points along the size-scale axis (the *x*-axis of Fig. 4a), reveal a marked (*P* < 0.001) discontinuity in *D* at areas around 60–70 ha. The discontinuity was signaled by a kink in the log *P* against log *A* plot. Small areas of forest tend to be smoother with *D* ≈ 1.20 ± 0.02, while larger areas, greater than 70 ha, have more complex boundaries, *D* ≈ 1.52 ± 0.02. This result is interpreted to indicate that human disturbances predominate at small scales making for smoother geometry and lower *D*, while natural processes (e.g. geology, distributions of soil types, etc.) continue to predominate at larger scales.

Scaling: persistence/smoothness

One of the more intriguing applications that has particular relevance to remote sensing studies concerns the connection (discussed in Box 3) between fractal spatial patterns and modified Brownian dynamics.

As outlined in Box 3, there are simple relationships between persistence, measured by the parameter *H* in modified Brownian diffusion models (see Box 3), and fractal exponents. Although the exact relationship between *H* and *D* depends on the details of the assumed model (Hastings and Sugihara, unpublished), the general relationship remains: increased persistence (more memory in the process) should correspond to smoother boundaries and patches with larger and more uniform areas;

whereas reduced persistence will correspond to more complex and highly fragmented landscapes dominated by many small areas. For example, in simple patch-extinction models[12], persistence in the dissemination of spatial displacements corresponds roughly with how long the resulting patches last. Given that for a particular natural landscape the Brownian paradigm is somewhat reasonable, one might expect to find the predicted relationship between reduced shape complexity and persistence in time. Indeed, without committing to any particular Brownian model, it may be possible to obtain a purely empirical scaling that relates a pattern's ephemerality to its fractal exponent, *D*.

Hastings *et al.*[12] have examined this possibility for patches of two kinds of vegetation, cypress and broadleaf, in the Okefenokee Swamp, USA. They fit patch areas to the hypergeometric distribution to determine *B* (Eqn 2), which is then used to estimate *H* and *D* (see previous section on hyperbolic distribution). Hastings *et al.* find that the fractal exponent *D* is larger (thus persistence, *H*, is lower) for the earlier successional cypress. The more persistent broadleaf vegetation which eventually dominates has a lower value of *D*. They speculate that *D* may be used as an index of succession in circumstances where simple patch-extinction models are reasonable.

Several additional anecdotes help to illustrate these ideas. An initial analysis of satellite ocean-color patterns appears to corroborate the predicted relationship between shape complexity and persistence (Sugihara, unpublished). The boundary-grid method applied to a series of images of the California Current taken by a remote color scanner reveals remarkably good fits to single fractal exponents on length scales between 1 km and 10000 km. When stable patterns of low productivity of typical years are compared with transient El Niño conditions, the predicted correlation between fragmentation and vagility is observed. Transient El Niño years show low and high productivity regions having a patchier and more highly dissected appearance than is the case in typical years.

Similar informal observations arise in the patch dynamics of sessile organisms. Healthy vestimentiferan reefs formed within plume fields of deep-sea hydrothermal vents often appear to have a much simpler geometry than failing colonies that inhabit vents on the verge of extinction (R. Hessler, pers. commun.). Similarly, certain persistent bryozoan and coral colonies (e.g. *Montipora* spp.) often have simpler outlines and are less patchy than colonies of more ephemeral species (e.g. *Pocillopora* spp.) (Ref. 21; T. Hughes, pers. commun.; J. Connell, pers. commun.). It would be interesting to follow up these provocative anecdotes with careful studies to determine to what extent *D* computed from snapshots can be used as an index of physiological state or persistence of patches in time, and how such persistence may relate to the spatial scales involved.

Extinction

Another potential application of fractals in ecology is to the related problem of persistence of rare species. Rather than focusing on spatial geometry, we shall consider instead the fractal properties of a time series of population values.

Viewed in the light of a modified Brownian model (Box 3), one might expect the range of values in a time series to grow roughly as time raised to the power *H* (i.e. $\triangle t^H$). That is, if $x(t)$ is the time series variable, and $x^*(t)$ is the normalized deviation $|x^*(t) = x(t) - \bar{x}(t)$ for *t* between 0 and *T*|, then the range $R(T)$ |where $R(T) = \max x^*(t) - \min x^*(t)$ for *t* between 0 and *T*| of a modified Brownian process will scale with the length of the time series, *T*, as

$$R(T) = cT^H \qquad (3)$$

According to the third equation in Box 3, the fractal exponent *D* for the time series is computed as $D = 2 - H$. Thus, Eqn 3 provides another method for calculating *D* for a time series. All that is required is a regression of log range against log time, and the resulting slope is *H*. Notice that when $H > 1/2$, the time series is smoothed out (lower value of *D*); but because the Brownian process is more persistent in its deviations, the time series goes through wider swings.

Such power-law scaling between

range and time has been observed empirically in river discharge records[16]. The values of *H* computed here have been found to vary between 1/2 and 1, indicating a tendency toward persistence in the fluctuations of river discharge, i.e. wet years tend to be followed by other wet years. Moreover, this persistence is scale-invariant in that the autocorrelation remains at all scales (at least at all scales used to measure *H*). That is, correlations between wet weeks will scale upward in a self-similar fashion to imply correlations between wet years and wet decades, etc. This information is important, for example, in designing a reservoir so that in its finite lifetime it will never overflow and never empty.

The analogy to populations is clear. All things being equal, a species whose population time series follows Eqn 3 would be more vulnerable to local extinction if its range of population values increases faster with time (larger *H*) than one whose population range grows only slowly (lower *H*). Roughly speaking, the time to extinction should scale as $c'N^{1/H}$, where c' is a constant less than 1 and *N* is the average population size. Thus, one may speculate that vulnerability to extinction should be associated with a larger *H* or a lower fractal exponent for the time series, whereas more stable species will have time series with a lower *H*.

Figure 5 shows an informal example of such an analysis for two bird species having roughly the same average abundance[22]. According to Eqn 3, the slope of the log *R* against log *T* plot yields a value for *H*. The value of *H* for the least flycatcher (*Empidonax minimus*) (*H* = 0.56) is higher than for the American redstart (*Setophaga ruticilla*) (*H* = 0.38), suggesting that the former is more prone to local disappearance and less subject to density-dependent population corrections. A lower *H* for the American redstart suggests anti-persistence in its time series (higher *D*), which again translates roughly to tighter density-dependent population correction.

Dimension and embedding

As a final suggestion for a possible class of applications of fractals that may be of interest to ecologists, we consider how the concept of di-
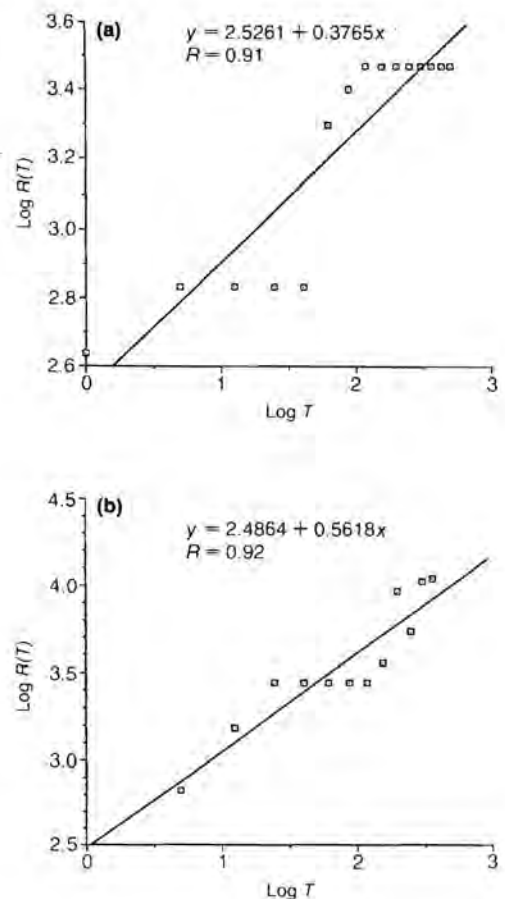

Fig. 5. Log range in population values (normalized, *R*(*T*) – see text) versus log time of observation (*T*) for two equally abundant bird species (time series data from Ref. 22). The slope yields a value of *H* from which *D* for the time series can be calculated as *D* = 2−*H*. (a) For the American redstart *H* = 0.38, and (b) for the least flycatcher *H* = 0.56. A higher value of *H* for the least flycatcher implies higher suceptibility to local extinction and weaker density-dependent control.

mension operates in sampling, i.e. why sweep nets should work better than flypaper.

Consider two sets of dimension D_m and D_p embedded in a space of dimension *E*. In order for them to intersect with nonzero measure, it is necessary that

$$D_m + D_p > E$$

Thus, a sampling scheme of dimension D_m used in a space of dimension *E* can only detect phenomena of dimension $D_p > E - D_m$.

Lovejoy et al.[23] discuss an application of this idea in connection with the ability of the worldwide network of fixed weather stations to detect weather phenomena of different dimension. They use a modification of the generalized grid method to obtain a value of $D_m = 1.75$ for the worldwide network of weather stations. Assuming *E* = 2, phenomena of dimension $D_p < 0.25$ cannot

be detected by this network. Apparently, the low-dimensional phenomena that might be missed characterize certain violent episodic storms – a good case for the use of satellites.

In addition to the possible, though perhaps only weak, relevance of these ideas for designing sampling regimes in ecology (e.g. for monitoring acid rain), they may be used to motivate a variety of interesting evolutionary hypotheses involving encounter rates (e.g. between predator and prey).

For example, in cases where a predator searches randomly (having no information about the whereabouts of its prey), one might expect selection to operate toward maximizing the dimensionality of the predator's search path. Thus, such predators may have highly convoluted and space-filling search trajectories. Prey movements, on the other hand, might tend to be simpler, or the prey may be distributed in space so as to minimize their dimension (Cowles and Sugihara, unpublished). It would be an interesting and workable task to investigate how dimensional considerations may come to play in evolution by maximizing or minimizing the frequency of different kinds of encounter.

Conclusion

Fractal scaling appears as a ubiquitous property of nature. It has some promise both as an economical description of natural patterns and, more speculatively, as a tool for probing causes. Whereas the formally defined Hausdorf dimension is not in itself usually a practical concept, in real applications the less stringent fractal exponent may prove to be more valuable. Moreover, because the mechanics of estimating fractal exponents are often straightforward, they should be particularly attractive as a novel way to approach some difficult problems involving scale and hierarchy in ecological systems. The suggestions for applying fractals that are offered above illustrate their potential interest in ecology.

References

1 Mandelbrot, B.B. (1977) Fractals: Form Chance and Dimension, W.H. Freeman & Co.
2 Barnsley, M.F., Ervin, V., Hardin, D. and Lancaster, J. (1986) Proc. Natl Acad. Sci. USA 83, 1975–1977
3 Falconer, K.J. (1985) The Geometry of Fractal Sets, Cambridge University Press
4 Lohle, C. (1983) Specul. Sci. Technol. 6, 131–142
5 Allen, T.F.H. and Starr, T.B. (1982) Hierarchy: Perspectives For Ecological Complexity, University of Chicago Press
6 Sugihara, G. (1984) in Exploitation of Marine Communities (May, R.M., ed.), pp. 131–153, Springer-Verlag
7 O'Neill, R.V., De Angelis, D.L., Waide, J.B. and Allen, T.F.H. (1986) A Hierarchical Concept of Ecosystems, Princeton University Press
8 O'Neill, R.V. et al. Landsc. Ecol. (in press)
9 Milne, B.T. Appl. Math. Comput. (in press)
10 May, R.M. (1989) in Ecological Concepts (Cherrett, J.M., ed.), pp. 339–363, Blackwell
11 Frontier, S. (1987) in Development in Numerical Ecology (Legendre, P. and Legendre, L., eds), pp. 335–378, Springer-Verlag
12 Hastings, H.M., Pekelney, R., Monticolo, R., Van Kannon, D. and DelMonte, D. (1982) BioSystems 15, 281–289
13 Gukenheimer, J. (1984) Contemp. Math. 28, 357–367
14 Korcak, J. (1938) Bull. Inst. Int. Stat. III, 295–299
15 Morse, D.R., Lawton, J.H., Dodson, M.M. and Williamson, M.H. (1985) Nature 314, 731–732
16 Mandelbrot, B.B. (1983) The Fractal Geometry of Nature, W.H. Freeman & Co.
17 Briand, F. and Cohen, J. (1987) Science 238, 956–960
18 May, R.M. (1983) Nature 301, 566–568
19 Krummel, J.R., Gardner, R.H., Sugihara, G. and O'Neill, R.V. (1987) Oikos 48, 321–324
20 Bradbury, R.H., Reichlet, R.E. and Green, D.G. (1984) Mar. Ecol. Prog. Ser. 14, 295–296
21 Jackson, J.B. and Hughes, T. (1985) Am. Sci. 73, 265–274
22 Holmes, R.T. and Sherry, T.W. (1986) Ecol. Monogr. 56, 201–220
23 Lovejoy, S., Scherter, D. and Ladoy, P. (1986) Nature 319, 43–44

Reviews Scheduled for Forthcoming Issues of *TREE*

* The control of vertebrate pests by vertebrate predators, *A. Newsome*
* The ecology and evolution of reproductive synchrony, *R.A. Ims*
* The evolution and adaptive significance of heterostyly, *S.C.H. Barrett*
* Microbial mats and the early evolution of life, *D.J. Des Marais*
* Forces maintaining genetic diversity at the major histocompatibility complex, *W.K. Potts and E.K. Wakeland*
* The genetics of transient populations: research at the metapopulation level, *I. Olivieri, D. Couvet and P-H. Gouyon*
* DNA and morphology in the inference of plant morphology, *K.J. Sytsma*
* Larval mortality and the composition of coral reef fish communities, *C.M. Roberts*
* Coral reef primary productivity: a hierarchy of pattern and process, *B.G. Hatcher*
* From ecosystems to genes: the importance of shade tolerance in plants, *F.I. Woodward*